ELSEVIER

Journal of Alloys and Compounds 234 (1996) 34–39

Journal of ALLOYS AND COMPOUNDS

# Phase relations in neptunium-rich binary alloys with chromium, manganese, cobalt and nickel

J.K. Gibson[a,*], R.G. Haire[a], Y. Okamoto[b], T. Ogawa[b]

[a]*Oak Ridge National Laboratory, P.O. Box 2008, Oak Ridge, TN 37831-6375, USA*
[b]*Japan Atomic Energy Research Institute, Tokai-mura, Ibaraki-ken, 319-11, Japan*

Received 20 June 1995; in final form 28 July 1995

**Abstract**

Differential thermal analysis (DTA) has been used to probe the essential phase relations in Np-rich binary alloys with selected 3d transition metals (TMs). DTA measurements were carried out on the following Np-rich alloys (aggregate compositions): $Np_{83}Cr_{17}$, $Np_{79}Mn_{21}$, $Np_{79}Co_{21}$ and $Np_{80}Ni_{20}$. The results suggest that the essential phase relations in these Np-rich alloys are similar to those in the corresponding U–TM and Pu–TM systems. Each of these Np–TM systems is apparently characterized by an Np-rich eutectic which occurs at a temperature intermediate between those of the corresponding Pu–TM and U–TM eutectics: $T_{eut}(Pu\text{–}TM) \leq T_{eut}(Np\text{–}TM) < T_{eut}(U\text{–}TM)$. The $Np(\alpha \rightarrow \beta)$ allotropic transformation was retained in these alloys at virtually the same temperature as in pure Np, while the $Np(\beta \rightarrow \gamma)$ transition in the alloys was depressed by between 6 °C (Np–Cr) and 42 °C (Np–Mn). The small shifts in the neptunium transition temperatures suggest minimal solubilities of these TMs in Np. Evidence for the existence of the previously reported intermetallic phases, $Np_6Mn$ and $Np_6Co$, was not observed in the DTA data, possibly reflecting slow formation kinetics.

*Keywords:* Binary alloys; Phase relations; Neptunium

## 1. Introduction

The alloying behavior of neptunium has received scant attention as compared with its technologically more important actinide (An) neighbors, uranium and plutonium. Even the basic features of several key binary neptunium alloy phase diagrams, including those with first-row transition metals (TMs), have not been characterized. In support of the development of advanced technologies for managing the substantial quantities of neptunium which have accumulated as fission reactor byproducts, additional knowledge of its fundamental interactions with the constituents of common structural and containment materials is needed [1]. The alloying behavior of Np is furthermore of fundamental scientific interest for illuminating the nature of intermetallic bonding, and particularly the role of the quasi-valence semilocalized 5f electrons which are unique to the actinides and exhibit a maximum bonding contribution for neptunum metal [2,3].

Given that Np remediation technologies will probably employ zirconium- and iron-based materials, we previously developed phase diagrams for the Np–Zr and Np–Fe systems based on the results of differential thermal analysis (DTA) and powder X-ray diffraction (XRD) studies [4–6]. The predicted correspondence of the Np–Zr diagram to the U–Zr and Pu–Zr diagrams was not entirely sustained by our experimental results; most notably, it was established that the Np solidus temperature was not substantially increased by the addition of Zr [4]. In the case of the Np–Fe system the DTA results [6] were more consistent with predictions, and indicated a phase diagram with transition parameters intermediate to those of the U–Fe and Pu–Fe systems, which exhibit similar diagrams to one another.

In the present work, we have initiated a project with the intent of obtaining key experimental information for binary alloys of neptunium with the 3d transition metals that neighbor Fe. Of particular interest was the effect of a transition metal on the phase behavior of neptunium. The initial series of DTA measurements,

* Corresponding author.

Elsevier Science S.A.
*SSDI* 0925-8388(95)02013-6

reported here, were carried out on Np-rich binary alloys with Cr, Mn, Co and Ni.

## 2. Experimental details

The DTA apparatus and procedures have been described in detail elsewhere [4]. The materials preparation and handling techniques were similar to those used successfully for the study of the Np–Fe system [6].

$^{237}$Np metal ($Np^0$) was obtained as an electrorefined product and analysis indicated metallic impurities of less than 200 wt.ppm. The transition metals ($TM^0$) each had a vendor-specified purity of at least 99.9%. Alloy specimens were prepared by repeatedly (six to eight times) arc melting weighed Np + TM mixtures. The following aggregate compositions (and total prepared masses) were studied: $Np_{83}Cr_{17}$ (306 mg), $Np_{89}Mn_{21}$ (229 mg), $Np_{89}Co_{21}$ (186 mg) and $Np_{80}Ni_{20}$ (407 mg). A small portion (less than 10%) of the total mass of each alloy preparation was withheld from the DTA samples for other analyses.

Thermal analyses were carried out in an argon atmosphere glove-box using a Perkin–Elmer DTA1700 analyzer; the maximum achievable temperature was about 1350 °C. The samples were contained in $Al_2O_3$ cups with tantalum lids, and were purged with argon during the DTA measurements. Previous work with pure Np showed alumina to be a suitable container material and visual inspection of the post-DTA samples in the present work also indicated that very little alloy–crucible reaction had occurred.

A standard heating rate of 10 °C $min^{-1}$ was used throughout these studies. Transition temperatures were derived from extrapolated peak onsets. Temperature calibration was achieved using pure metals, $Al^0$, $Cu^0$ and $Mn^0$ [7], and the reported alloy transition temperatures are considered accurate to ±5 °C; the precision was sufficient to compare relative temperatures with a reliability of ±3 °C. Transition enthalpies could be derived from peak areas with an accuracy of about ±30%; the relative enthalpy values of the transitions exhibited by a specimen were generally more reliable than the absolute values, and the former were primarily considered in interpreting the DTA results.

## 3. Results and discussion

### 3.1. General

Representative DTA heating curves obtained for the four alloys studied are shown in Figs. 1–4 (downward peaks are endothermic transitions) and the results are summarized in Table 1. Each alloy was investigated up to a temperature of at least 1050 °C (higher when instrumental stability allowed). For none of the alloys investigated were reversible transitions identified above 620 °C. At lest two DTA heating curves were obtained for each alloy to confirm that the observed transitions were reproducible and reversible and that equilibrium had been achieved. If minor changes were noted between thermograms for an alloy specimen, the analysis was repeated until reproducible results were obtained; the reported thermograms are thus for alloy specimens which were "heat treated" in situ after their preparation by arc melting. Cooling curves confirmed the reversibility of the transitions identified during the heating portion of the analyses.

Table 1
Primary differential thermal analysis peaks for Np-rich Np–TM alloys[a]

| | Peak a | Peak b | Peak c |
|---|---|---|---|
| $Np_{83}Cr_{17}$ (Fig. 1) | 277 | 572; 73 | 619; 78 |
| $Np_{79}Mn_{21}$ (Fig. 2) | 276 | 536; 139[b] | |
| $Np_{79}Co_{21}$ (Fig. 3) | 277 | 566; ≈75 | 608[c]; ≈75 |
| $Np_{80}Ni_{20}$ (Fig. 4) | 274 | 551 | 590[c] |
| | | $\Delta H$(b + c) = 370 | |
| Pure $Np^0$ (Ref. [8]) | 282 | 578; 59 | 640[c]; 64 |
| | (α→β) | (β→γ) | (γ→iq) |

[a] Peaks a, b, c are labeled in Figs. 1–4. The data are presented as follows: $T_{onset}$ (°C); $\Delta_{tr}H$ for peaks b and c normalized to $\Delta H$(peak a) = 100.
[b] Triplet.
[c] Broad liquidus transition ($T_{onset} \neq T_{tr}$).

The principles used in this work for interpreting the DTA results to ascertain alloy phase equilibria have been described in general by others [9]. Transition temperatures were derived from the extrapolated onset temperatures of heating curve endotherms. The relative enthalpies associated with the endothermic alloy transitions were obtained from the ratios of their peak areas. The reported transition temperatures are most accurate when directly compared with those obtained under comparable experimental conditions; accordingly we compare the present results with those obtained previously in our laboratory for pure $Np^0$ [8].

The initial series of DTA measurements on selected Np–TM alloys reported here provide a survey of the essential natures of the Np-rich portions of the individual phase diagrams. Comparison with the corresponding U–TM and Pu–TM phase diagrams provides a basis for interpreting our Np–TM DTA results. Phase relations have not been established previously for these Np–TM systems, but the intermetallic compounds $Np_6Mn$ and $Np_6Co$ (as well as $Np_6Fe$) have been identified in XRD studies [10]. The Np–Cr phase diagram has been predicted based on the empirically determined An-rich portions of the U–Cr and Pu–Cr diagrams [11].

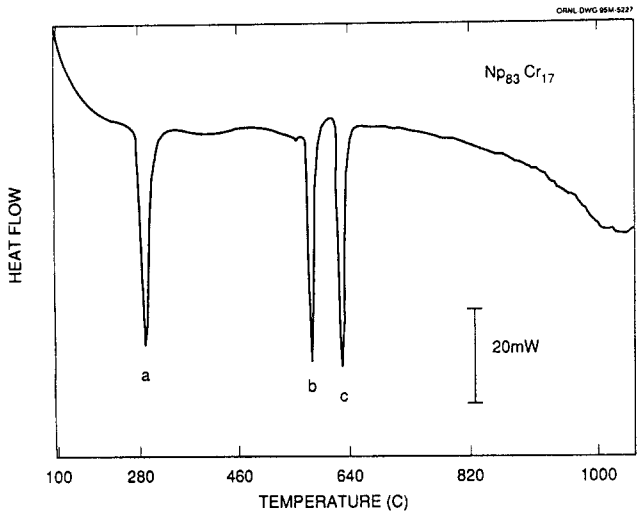


Fig. 1. Thermogram for $Np_{83}Cr_{17}$.

### 3.2. Neptunium–chromium

The thermogram obtained for the $Np_{83}Cr_{17}$ alloy (Fig. 1) is very similar to that for pure $Np^0$. Peaks in close correspondence to the three transitions established for pure $Np^0$, $\alpha \rightarrow \beta$ (peak a), $\beta \rightarrow \gamma$ (peak b) and $\gamma \rightarrow$ liquid (peak c), were evident; the relative enthalpy values were in reasonable accord with those for elemental $Np^0$ (Table 1). The two allotropic transitions for the Np–Cr alloy may have occurred at slightly (about 5 °C) lower temperatures than for pure Np; the solid ($\gamma$) → liquid transition temperature was more substantially depressed, by about 20 °C. The results suggest that the Np–Cr phase diagram is similar to those of the U–Cr and Pu–Cr systems, both of which exhibit negligible solid solubilities, no intermediate phases and an An-rich eutectic [11]. A particular similarity of the Np–Cr system to the U–Cr system had been predicted [11], but the present results suggest that $T_{eut}$(Np–Cr) = 619 °C, which is essentially identical to $T_{eut}$(Pu–Cr) = 620 °C. Venkatraman et al. [11] noted that their thermodynamic model of An–Cr systems generally predicted eutectic temperatures lower than those observed; it is consistent that their speculative Np–Cr phase diagram gives a eutectic temperature of 503 °C in contrast to our experimentally determined value of 619 °C. Based on the retention of the $\beta \rightarrow \gamma$ allotropic transition in the alloy, it can be concluded that the Np–Cr eutectic reaction corresponds to $L \rightarrow Cr\{Np\} + \gamma\text{-}Np\{Cr\}$ (M{M′} designates a solution of M′ in M); β-Np{Cr} had been predicted for this reaction [11]. The large enthalpy of the Np–Cr eutectic transition (peak c) suggests a composition $X_{eut}$(Np–Cr) (atomic percentage of Np, with the balance Cr) near that of the alloy sample, i.e. $X_{aggregate}$ = 83 at.% Np–Cr, which is closer to $X_{eut}$(U–Cr) = 81 at.% than to $X_{eut}$(Pu–Cr) ≈ 99 at.% Pu. The slight downward slope of the Np–Cr thermogram above 600 °C may reflect hypereutectic fusion of residual solid (e.g. $Cr\{Np\} \rightarrow L$, assuming $X_{eut}$(Np–Cr) > 83 at.% Np); however, this curve shape may rather reflect a poor baseline, and indeed DTA data above 1050 °C were not obtained for this sample owing to pronounced instrumental instabilities at higher temperatures.

### 3.3. Neptunium–manganese

All of the thermograms obtained for $Np_{79}Mn_{21}$ exhibited a singlet peak (a) and a triplet peak (b) shown in Fig. 2. Anomalous features, such as the exotherm at about 700 °C in Fig. 2, were occasionally evident at higher temperatures but were neither reproducible nor attributed to reversible alloy transitions. Peak a corresponds closely to the elemental $Np(\alpha \rightarrow \beta)$ allotropic transition. The magnitude (area) of triplet b is such that it apparently comprises the enthalpy associated with both the $Np(\beta \rightarrow \gamma)$ and the $Np(\gamma \rightarrow$ liq) transitions. The first (and largest) peak in the triplet (peak b-1) is attributed to the $Np\{Mn\}(\beta \rightarrow \gamma)$ allotropic transition at 536 °C, which is about 42 °C below the corresponding transition temperature for pure $Np^0$ [8]; this decrease is greater than observed for the $Np\{Cr\}(\beta \rightarrow \gamma)$ transition but is still small enough to suggest limited Mn-in-Np solid solubility. Peak b-2 at about 560 °C is then assigned to the Np–Mn eutectic and the slightly broader peak, b-3, to post-eutectic fusion of residual solid. Both the U–Mn [12] and Pu–Mn [13, pp. 609–610] phase diagrams are characterized by an An-rich (more than 75 at.% An) eutectic. The eutectic enthalpy (b-2) was not accurately assessed but it appeared to be somewhat

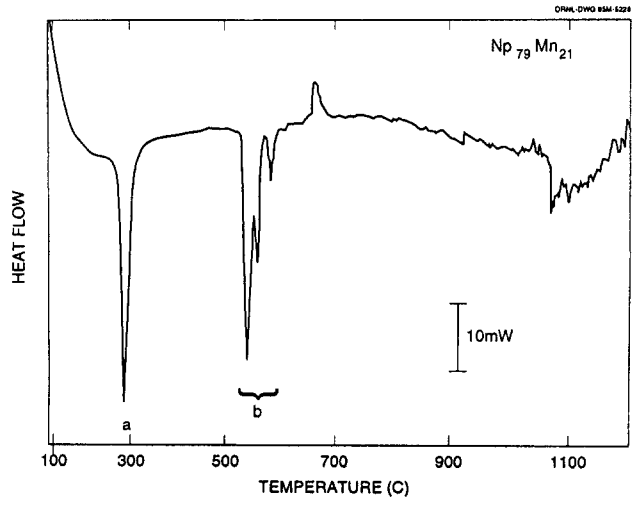


Fig. 2. Thermogram for $Np_{79}Mn_{21}$.

greater than that associated with the subsequent incongruent melting (b-3), suggesting $X_{eut}(Np–Mn) \approx 86 \pm 4$ at.% Np–Mn, which is comparable with the Pu–Mn system, where $X_{eut}(Pu–Mn) = 89$ at.% Pu.

Both $PuMn_2$ and $UMn_2$ are known intermetallic compounds, which melt congruently above 1000 °C [12, 13, pp. 609–610]; therefore, a corresponding $NpMn_2$ phase can be predicted with confidence. In contrast to the stable $AnMn_2$ phases, the compound $U_6Mn$ decomposes peritectically at 726 °C while $Pu_6Mn$ has not been identified [12,13, pp. 609–610]; $Np_6Mn$ was prepared by annealing at 600 °C an arc-melted alloy [10]. The strong Np{Mn}($\alpha \rightarrow \beta$) transition (peak a in Fig. 2), which was unchanged in subsequent DTA runs after in situ heating to 1200 °C, indicated that $Np_6Mn$ was not substantially produced in the present work, and it is possible that this intermetallic phase is only marginally stable.

Although the intense DTA peak corresponding to the Np($\alpha \rightarrow \beta$) transition indicates minimal formation of $Np_6Mn$, alternative peak assignments could otherwise explain the high temperature DTA results. For example, the following assignments are suggested by analogy with the U–Mn system: b-1, $Np_6Mn + NpMn_2 \rightarrow L$ (eutectic); b-2, $Np_6Mn \rightarrow L + \beta$-Np{Mn} (peritectic); b-3, $\beta$-Np{Mn} $\rightarrow \gamma$-Np{Mn}. It is re-emphasized that the apparently substantial amount of $\alpha$-Np{Mn} in the DTA specimens refutes the major role of $Np_6Mn$ implicit in these assignments.

### 3.4. Neptunium–cobalt

The thermograms for $Np_{79}Co_{21}$ were characterized by three major peaks, a, b and c, shown in Fig. 3. The small sharp feature on the high temperature edge of peak b was reproducible; it was more pronounced during the initial heating cycles. As with the other Np–TM alloys studied in the present work, peak a

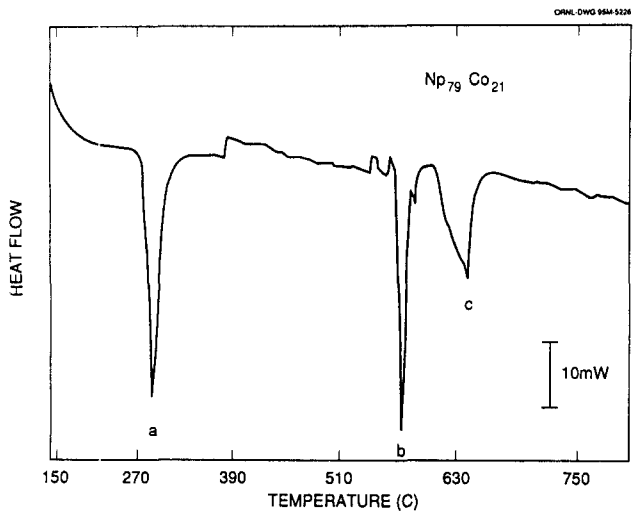


Fig. 3. Thermogram for $Np_{79}Co_{21}$.

(277 °C) closely coincided with the Np°($\alpha \rightarrow \beta$) transition, and the presence of this intense Np transition suggests that the intermetallic phase, $Np_6Co$, was not substantially formed. Peak b is indicative of the Np{Co}($\beta \rightarrow \gamma$) transition, which was depressed by about 10 °C relative to $Np^0(\beta \rightarrow \gamma)$. The broad shape of peak c suggests a solid–liquid melting curve which terminates at about 660 °C. Consistently with these interpretations, the small shoulder peak on the high temperature side of peak b, at about 585 °C, is then assigned to the eutectic. The relatively large magnitude of the post-eutectic transition (peak c) suggests that much of the sample melted along the liquidus curve, and thus that the value of $X_{eut}(Np–Co)$ is substantially different from the aggregate sample composition of 79 at.% Np–Co (e.g. $X_{eut}(Np–Co) <$ 74 or >84 at.% Np). The eutectic compositions for the corresponding U–Co and Pu–Co systems are about 62 at.% U and about 87 at.% Pu. The measured $T_{eut}(Np–Co) \approx 585$ °C is intermediate between $T_{eut}(U–Co) \approx 740$ °C and $T_{eut}(Pu–Co) \approx 400$ °C.

In contrast to the other alloys studied, the Np–Co sample was characterized by significant thermal hysteresis effects, and the results discussed above (and shown in Fig. 3) correspond to thermograms obtained after repeated heating–cooling cycles. The most notable variation in the thermograms was the diminution (especially after relatively rapid cooling) of an additional peak at about 540 °C which had been a significant feature of the initial Np–Co thermograms (and is not clearly evident in Fig. 3). This transitory peak may have corresponded to the decomposition of a marginally stable intermediate phase (perhaps $Np_6Co$) whose formation may be highly sensitive to thermal treatment conditions (specifically, the cooling rate). The observed onset temperature of about 540 °C for this intermittent Np–Co transition can be compared with reported decomposition temperatures of about 400 °C for $Pu_6Co$ (close to $T_{eut}(Pu–Co)$) and about 840 °C for $U_6Co$ [13, pp. 329–331 and 341].

As with the Np–Mn system, were it not for the intense Np($\alpha \rightarrow \beta$) peak (which refutes the presence of $Np_6Co$), the high temperature DTA features might be satisfactorily explained by a phase diagram similar to the U–Co diagram. Specifically, peak b could otherwise be assigned to a peritectic decomposition of $Np_6Co$ and peak c to a post-peritectic liquidus curve.

### 3.5. Neptunium–nickel

The thermograms for the $Np_{80}Ni_{20}$ specimen were also characterized by three main peaks, a, b and c, as shown in Fig. 4. In similarity to the Np–Co system (Fig. 3), the small spike between peaks b an c was also reproducible; in contrast to the Np–Co DTA results, substantial thermal hysteresis was not evident for the

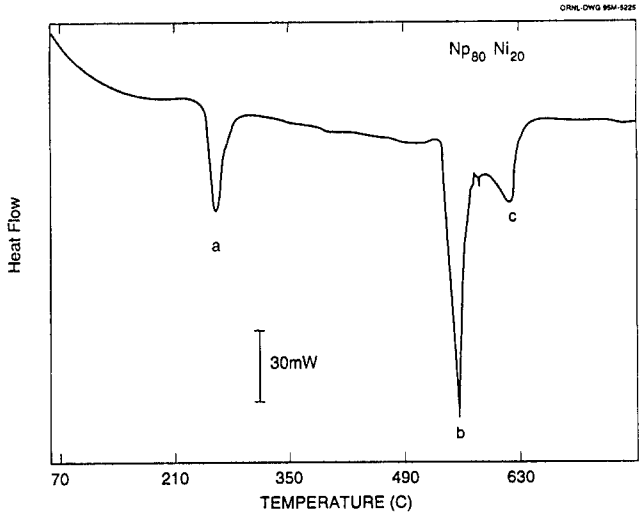


Fig. 4. Thermogram for $Np_{80}Ni_{20}$.

Np–Ni sample. Peak a apparently corresponds to the Np{Ni}(α→β) allotropic transition, depressed by 8 °C relative to the value for pure $Np^0$. In contrast to the other three Np–TM alloys, the enthalpy associated with the α→β transition (per mole of Np) was significantly (at least 30%) smaller than that for pure $Np^0$, suggesting that there had been substantial incorporation of Np into a second phase, perhaps NpNi (by analogy with PuNi [14]). The apparent absence of $Np_6Ni$, indicated by the retention of a substantial α→β transition, contrasts with the U–Ni system but accords with the Pu–Ni system and the Np–Ni XRD results of Giessen et al. [10].

Peak b in Fig. 4 is assigned to an Np{Ni}(β→γ) transition, which is depressed by about 30 °C relative to pure $Np^0$. The broad shape of peak c is indicative of melting over the approximate range 600–630 °C. The small sharp feature between peaks b and c, at about 580 °C, is attributed to the Np–Ni eutectic; this eutectic temperature can be compared with $T_{eut}$(U–Ni) = 740 °C [14] and $T_{eut}$(Pu = Ni) = 465 °C [15]. The large area of the Np–Ni liquidus (peak c) suggests that the eutectic composition $X_{eut}$(Np–Ni) is substantially discrepant from the alloy composition of 80 at.% Np (e.g. $X_{eut}$(Np–Ni) < 75 or >85 at.% Np); for comparison, $X_{eut}$(U–Ni) = 67 at.% U [15] and $X_{eut}$(Pu–Ni) = 88 at.% Pu [14].

## 4. Conclusion

The key features of the Np-rich portions of the Np–TM phase diagrams inferred from our DTA results are summarized in Table 2. Each of the four diagrams would appear to be similar to the corresponding U–TM and Pu–TM diagrams. Both the Np(α→β) and the Np(β→γ) allotropic transformations were evident for each Np{TM} terminal solid solution, which apparently formed as the dominant phase for each of the specimens studied. Relative to pure $Np^0$, $T_{tr}$(α→β) and $T_{tr}$(β→γ) for the alloys were slightly depressed (by less than 10 °C and less than 50 °C respectively), suggesting limited TM-in-Np solid solubilities. The effect of Cr on the Np allotropic transition temperatures was minimal, indicating a particularly small solubility of Cr in Np, consistent with the limited solubilities in the U–Cr and Pu–Cr systems.

For each of the four Np–TM alloy systems, an Np-rich eutectic was identified at a temperature intermediate between the corresponding U–TM and Pu–

Table 2
Key features of An–TM phase diagrams[a]

| An–TM system | Intermediate phases | An-rich eutectic | |
|---|---|---|---|
| | | $T$ (°C) | $X$ [An] (at.%)[b] |
| U–Cr | None | 860 | 81 |
| Np–Cr | (None?) | 619 | >76, <90 |
| Pu–Cr | None | 620 | 99 |
| U–Mn | $U_6Mn$, $UMn_2$ | 716 | 79 |
| Np–Mn | $Np_6Mn$[c], ($NpMn_2$?) | 560 | >82, <90 |
| Pu–Mn | $PuMn_2$ | 520 | 89 |
| U–Co | $U_6Co$, UCo, $UCo_2$, etc. | 740 | 62 |
| Np–Co | $Np_6Co$[c] (etc.?) | 585 | <74, or >84 |
| Pu–Co | $Pu_6Co$, $Pu_3Co$, $Pu_2Co$, etc. | 406 | 87 |
| U–Ni | $U_6Ni$, $UNi_2$, etc. | 740 | 67 |
| Np–Ni | (NpNi, etc.?) | 580 | <75 or >85 |
| Pu–Ni | PuNi, $PuNi_2$ | 465 | 88 |

[a] U–TM and Pu–TM references are in the text; all terminal TM-in-An solid solubilities are small.
[b] $X_{eut}$(Np–TM) estimated from eutectic vs. liquidus enthalpies.
[c] Reported in Ref. [10]; however, not clearly indicated by DTA.

TM eutectic temperatures (although $T_{eut}$(Np–Cr) ≈ $T_{eut}$(Pu–Cr)]. The Np–TM eutectic reactions can be generalized as $L \rightarrow \gamma\text{-Np}\{TM\} + TM_xNp_y$, where the latter is a relatively TM-rich phase (e.g. presumably $y \approx 0$ for TM = Cr). Although approximate eutectic composition ranges or limits could only be inferred, the results were in general qualitatively consistent with $X_{eut}$(Np–TM) which were between the corresponding values for $X_{eut}$(U–TM) and $X_{eut}$(Pu–TM). No thermal effects distinctly attributable to intermediate phase formation were identified for any of the Np–TM systems examined; the apparent absence of significant amounts of two reported compounds, $Np_6Mn$ and $Np_6Co$, suggests that their formation may be kinetically hindered.

The primary conclusion derived from the present results is that the Np-rich portions of the Np–Cr, Np–Mn, Np–Co and Np–Ni phase diagrams are fundamentally similar, and generally intermediate, to the corresponding U–TM and Pu–TM systems. Specifically, each of these Np–TM phase diagrams appears to be characterized by an Np-rich eutectic and limited terminal TM-in-Np solid solubility.

Many U–TM and Pu–TM (and Np–TM) systems exhibit distinctive intermetallic phases; the present results reflect the particular difficulties which may be encountered in characterizing elusive intermediate phases with limited thermodynamic stability, such as $Np_6TM$. In conjunction with elaborated DTA investigations of these alloy systems, powder XRD of these and additional alloys, of different compositions and/or using other preparative conditions, are being pursued to probe more completely the intermediate phases and to clarify further the phase relations indicated by the preliminary DTA results reported here. Although the present Np–Cr and Np–Ni results were relatively definitive and in accord with other work and the corresponding U–TM and Pu–TM systems, the Np–Mn and Np–Co results were less conclusive and the latter systems must be further investigated to confirm the present interpretations.

## Acknowledgements

This work was sponsored by the Division of Chemical Sciences, Office of Basic Energy Sciences, US Department of Energy, under Contract DE-AC05840R21400 with Lockheed Martin Energy Systems, Inc. (LMES) and by the Japan Atomic Energy Research Institute (JAERI) under the Japan–US Actinide Program. The authors are grateful for the ongoing contributions and support of actinide alloy studies by Drs. T. Mukaiyama of JAERI and S. Raman of LMES.

## References

[1] E.K. Hulet, *Report of a Workshop on Transactinium Science, Rep. UCRL-LR-104538*, 1990, pp. 87–107 (Lawrence Livermore National Laboratory).
[2] T. Ogawa, *J. Alloys Comp., 194* (1993) 1.
[3] T. Ogawa, J.K. Gibson, R.G. Haire, M.M. Gensini and M. Akabori, *J. Nucl. Mater.*, in press.
[4] J.K. Gibson and R.G. Haire, *Thermochim. Acta, 207* (1992) 65.
[5] (a) J.K. Gibson and R.G. Haire, *J. Nucl. Mater., 201* (1993) 225. (b) M.M. Gensini, R.G. Haire and J.K. Gibson, *J. Alloys Comp., 213–214* (1994) 402.
[6] J.K. Gibson, R.G. Haire, E.C. Beahm, M.M. Gensini, A. Maeda and T. Ogawa, *J. Nucl. Mater., 211* (1994) 215.
[7] O. Kubaschewski, C.B. Alcock and P.J. Spencer, *Materials Thermochemistry*, Pergamon, New York, 1993, pp. 257–323.
[8] J.K. Gibson and R.G. Haire, *J. Nucl. Mater., 195* (1992) 156.
[9] D.E. Etter, P.A. Tucker and L.J. Wittenberg, in R.F. Schwenker and P.D. Garn (eds.), *Thermal Analysis*, Vol. 2, Academic Press, New York, 1969, pp. 829–850.
[10] B.C. Giessen, R.B. Roof, A.M. Russell and R.O. Elliott, *J. Less-Common Met. 53* (1977) 147.
[11] M. Venkatraman, J.P. Neumann and D.E. Peterson, *Bull. Alloy Phase Diag., 6* (1985) 418.
[12] M. Hansen, *Constitution of Binary Alloys*, McGraw-Hill, New York, 2nd edn., 1958, pp. 960–962.
[13] R.P. Elliott, *Constitution of Binary Alloys*, First Supplement, McGraw-Hill, New York, 1965.
[14] D.E. Peterson, *Bull. Alloy Phase Diagr., 9* (1988) 483.
[15] J.D. Grogan and R.J. Pleasance, *J. Inst. Met., 82* (1953) 141.